



Advances in the hydrodynamics solver of CO5BOLD

Bernd Freytag¹

Centre de Recherche Astrophysique de Lyon, UMR 5574: CNRS, Université de Lyon, École Normale Supérieure de Lyon, 46 allée d'Italie, F-69364 Lyon Cedex 07, France
e-mail: Bernd.Freytag@ens-lyon.fr

Abstract. Many features of the Roe solver used in the hydrodynamics module of CO5BOLD have recently been added or overhauled, including the reconstruction methods (by adding the new second-order “Frankenstein’s method”), the treatment of transversal velocities, energy-flux averaging and entropy-wave treatment at small Mach numbers, the CTU scheme to combine the one-dimensional fluxes, and additional safety measures. All this results in a significantly better behavior at low Mach number flows, and an improved stability at larger Mach numbers requiring less (or no) additional tensor viscosity, which then leads to a noticeable increase in effective resolution.

Key words. Stars: atmospheres – Numerical methods: hydrodynamics

1. Introduction: Previous and ongoing projects

The radiation-magneto-hydrodynamics code CO5BOLD is tailored to account for the conditions in the atmospheres of cool stars and sub-stellar objects, as well as the convective surface layers below (Freytag et al. 2012). There are separate modules for solving the hydrodynamics equations (with an approximate Riemann solver of Roe type, see Roe 1986) and the magneto-hydrodynamics equations (with an HLL solver, see Harten et al. 1983). Both account for ionization effects, gravity, and compressibility. There are two different geometrical setups: the one for local “box-in-a-star” models of a small patches of the stellar surface requires the use of the “MSrad” radiation transport module, that uses a long-

characteristics Feautrier scheme and accounts for horizontally periodic boundary conditions (e.g., Steffen et al. 2009; Ludwig & Kučinskas 2012). The other one is intended for performing global “star-in-a-box” simulations of (essentially) the entire stellar envelope and uses a short-characteristics scheme (“SHORTrad” module, see e.g., Freytag et al. 2002; Freytag & Höfner 2008). Both account for non-local radiation-transport, i.e., optically thin or thick conditions, and frequency-dependent opacities via an opacity-binning scheme. Various optional modules account for molecule or dust formation (e.g., Freytag & Höfner 2008; Freytag et al. 2010).

While CO5BOLD has simulated successfully the atmospheric flows in objects from A-type stars to brown dwarfs and from white dwarfs to red supergiants (Freytag et al. 2012),

Send offprint requests to: B. Freytag

a number of issues that ask for improvements have become apparent:

In Beeck et al. (2012), where solar models computed with the CO5BOLD, MURaM, and Stagger codes were compared, the CO5BOLD model has the lowest resolution, partly due to the relatively coarse grid but partly also due to the resolution-controlling settings. While Beeck et al. (2012) demonstrate that the choice of code and resolution hardly makes any difference for many important averaged quantities, there are cases where resolution does matter: Steffen et al. (2009) find that the microturbulence in the CO5BOLD atmospheres is lower than observed (see also Steffen, these proceedings).

Low-Mach-number flows (around and below $M=0.01$) show a comparably strong dissipation particularly of motions not aligned with the grid axes. In addition, the entropy could “misbehave” (see Fig. 5, top) and spurious pressure waves could occur in (nearly) incompressible flows. This is visible in the coolest brown-dwarf models in Freytag et al. (2010) or Freytag et al. (2011) and finally limited the model range to effective temperatures above 1000 K.

Possible problems at high Mach numbers on the other hand, like the non-circularity of the velocity in the classical Sedov blast-wave problem and some artefacts in the entropy field, were cured by the introduction of a tensor viscosity in addition to the built-in dissipation of the Roe solver. Some issues with the not exact conservation and the spurious transport of angular momentum in rotating global models were discussed in Steffen & Freytag (2007).

Examples how many these issues have been addressed in the current stable version “002.02.2012.11.05b” will be presented in the following.

2. Numerical dissipation

2.1. The need for numerical dissipation

The 1D linear advection equation

$$\frac{\partial q}{\partial t} = -v \frac{\partial q}{\partial x} \quad (1)$$

in one spatial coordinate x for the evolution of a scalar q in time t is a special case of the 3D Euler equations and has the general solution

$$q(x, t) = q(x - v(t - t_0), t_0) , \quad (2)$$

which means that the initial conditions at t_0 are transported (“advected”) with constant speed v without modifying them otherwise. This works even for non-continuous initial conditions.

Now, consider a discretization with equidistant steps Δx and Δt in space and in time, respectively. Ideally, any initial condition should be identically shifted for $\Delta t = n/v \Delta x$, $n \in \mathbb{N}$. But what happens for non-integer steps, e.g., for $\Delta t = 1/(2v) \Delta x$? A step function will be smoothed like

$$0, 0, 0, 1, 1, 1 \rightarrow 0, 0, 0, 1/2, 1, 1 \quad (3)$$

and a high-frequency wave will become

$$-1, 1, -1, 1, -1, 1 \rightarrow 0, 0, 0, 0, 0, 0 . \quad (4)$$

The discrete version of Eq. (1) behaves approximately as if there had been an artificial diffusive term added to the continuous equation, resulting in the modified equation

$$\frac{\partial q}{\partial t} = -v \frac{\partial q}{\partial x} + D \frac{\partial^2 q}{\partial x^2} . \quad (5)$$

This term is hardly avoidable for the highest-frequency fluctuations. However, it is well justified by upwind considerations. It can be further motivated by considering real physical diffusion at very small scales described by the Navier-Stokes equations that include viscous terms (and heat conduction).

2.2. Higher-order reconstruction

In contrast to dissipation on the smallest-scales, the dissipation of larger structures (for instance, sine waves with wavelengths significantly larger than $2\Delta x$) can be drastically reduced by an appropriate reconstruction scheme (see, e.g., van Leer 1979). While an *interpolated* function usually goes through the interpolation points but does not take these points in its integral into account, a *reconstructed* function in a grid cell has the grid value as integral

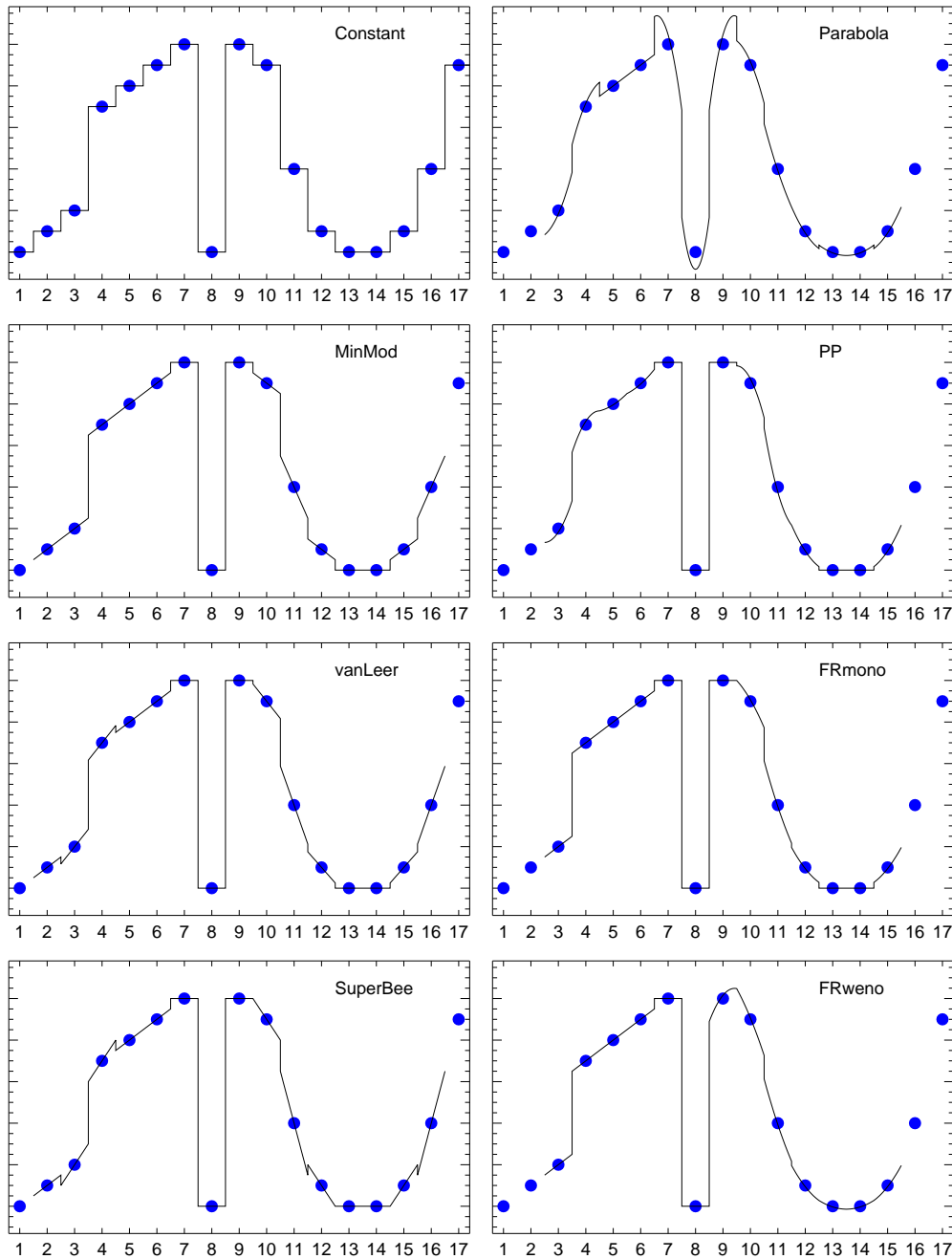


Fig. 1. Various reconstruction schemes for a small vector of points (filled circles): 0.0, 0.1, 0.2, 0.7, 0.8, 0.9, 1.0, 0.0, 1.0, 0.9, 0.4, 0.1, 0.0, 0.0, 0.1, 0.4, 0.9 using zero- or first-order polynomials (left column) or second-order polynomials (right column). Note, that only the “parabola” and the “FRweno” scheme show some overshoot (e.g., in cells 9 and 10), in contrast to the other – monotonic – schemes.

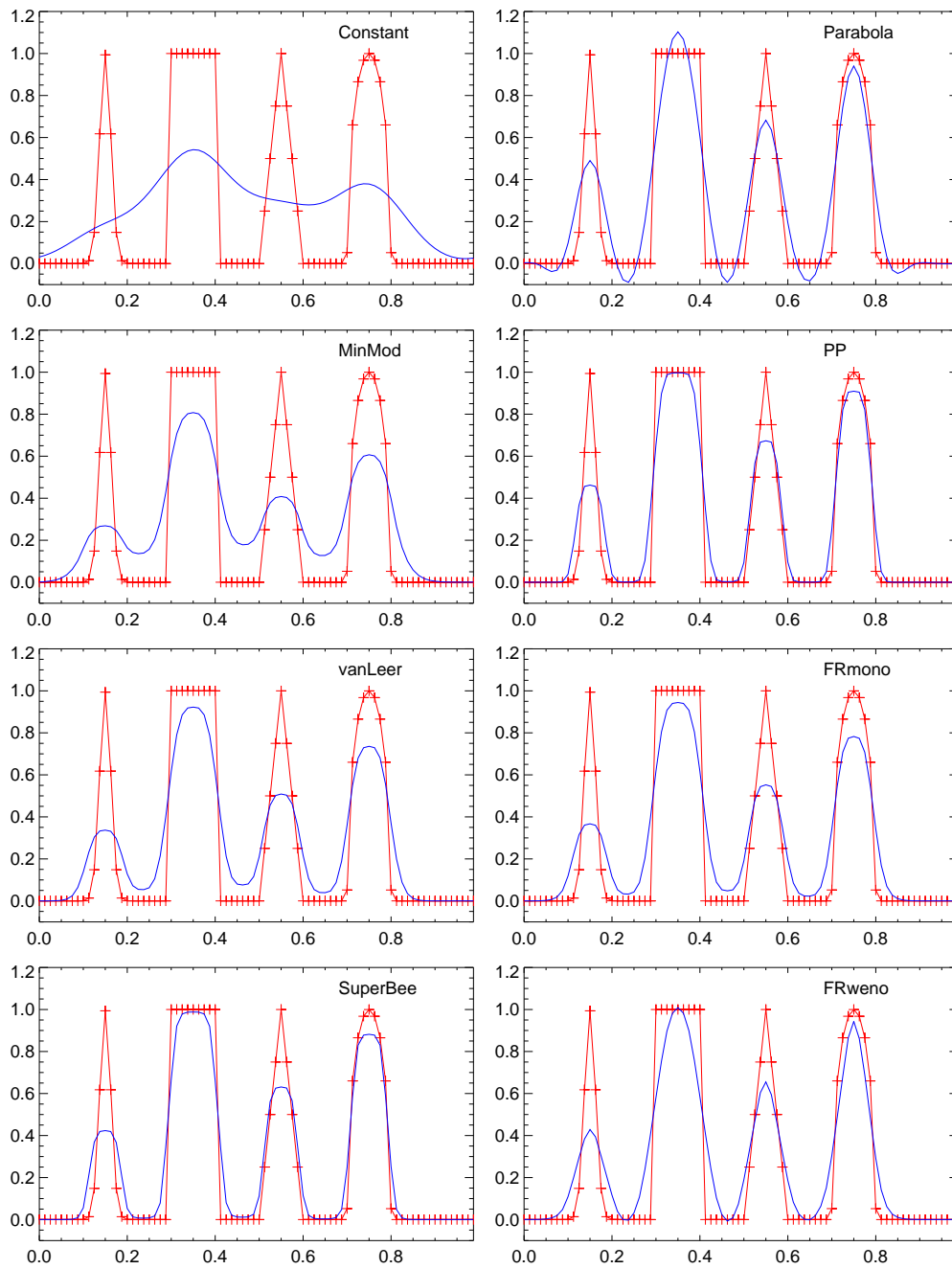


Fig. 2. Linear advection of the Shu & Osher spikes (red curves with plusses) after one revolution (black curves) using various reconstruction schemes (the same as in Fig. 1). The “Constant” scheme is highly diffusive, the “SuperBee” scheme transforms all shapes into smoothed rectangles, and the “Parabola” scheme has lots of overshoot. The other schemes are rather well behaved.

over the cell but does not necessarily adopt this value in the cell center. It might have discontinuities at cell boundaries, which the hydrodynamics solver has to account for. To get a higher-order reconstruction the value in each cell as well as in its neighbors are taken into account. Reconstructed functions are more appropriate for finite volume methods.

Once a reconstruction scheme is formulated, one can immediately derive a numerical solution method for the 1D linear advection Eq. (1) by performing for each time step:

1. A *reconstruction* step based on the discrete grid-cell values to get the continuous density function within all grid cells.
2. A transport or *advection* step by computing the *exact* solution of Eq. (2) for the continuous function.
3. A *restriction* step by integrating the advected (shifted) continuous function over the grid cell intervals to get discrete cell values back.

In Fig. 1 the result of several reconstruction schemes for a vector of grid-cell values is compared. All of those schemes except the “Parabola” are implemented in CO5BOLD. The result of advecting four “spikes” (Shu & Osher 1989) represented with 80 grid points after one cycle and 160 time steps is shown in Fig. 2.

A zeroth-order reconstruction with a constant results in the donor-cell scheme and is so diffusive that it is hardly of any practical use.

The first-order schemes MinMod, vanLeer, and SuperBee are significantly less diffusive and vanLeer has been the default for simulations with CO5BOLD for years. The reconstruction of a discrete density by a linear function with MinMod can be outlined as follows:

1. At each cell boundary, compute preliminary boundary values by simply averaging the values from the left and right neighbor cells.
2. In each cell, compute two candidate slopes from the cell density and each of the two boundary values.
3. If the slopes have a different sign, use an overall slope of zero.

4. Otherwise, use the slope with the minimum absolute value.

The larger the discontinuities in the reconstruction, the larger the diffusion. If the step across the discontinuity has the same sign as the step in the corresponding cell values (e.g., vanLeer scheme between cell 6 and 7) the diffusion actually smoothes the profile with time. However, if the steps have opposite sign (e.g., vanLeer scheme between cell 4 and 5) the resulting anti-diffusion can result in steepening. This is the reason why the SuperBee scheme has a comparably low overall dissipation of the initial structures in Fig. 2. The drawback of this property is that all the different initial shapes will turn into slightly smoothed rectangles with time. It is therefore not recommended for simulations with CO5BOLD. While the vanLeer reconstruction has anti-diffusion to a lesser degree, the MinMod scheme is completely free of it – at the cost of being noticeably more diffusive than the vanLeer scheme.

All the four above schemes are monotonicity preserving. They properly reduce their slopes at local extrema preventing any overshoot but also leading to diffusion and somewhat flattened tops in Fig. 2. That is not the case for the “Parabola” scheme, that simply computes a second-order polynomial from each cell value and its two immediate neighbors – therefor still requiring only a 3-point stencil. However, the resulting overshoot is usually not acceptable and more sophisticated second-order schemes are necessary.

The Piecewise Parabolic Method (PPM, see Colella & Woodward 1984) is one of those. However, the name “PPM” usually refers to the the complete hydrodynamics scheme (including the Riemann solver) they presented. I will use “PP” to refer to the reconstruction only. The reconstruction of a density by a parabola with the PP method using a 5-point stencil can be outlined as:

1. At each cell boundary, compute preliminary boundary values by a clever high-order average of the four neighbor cells (two at each side).

2. Make sure that the boundary values lie between the values of the immediate neighbors.
3. If a cell has a local extremum in the discrete cell values, use a constant value as reconstruction in the cell.
4. Otherwise, compute in the cell a candidate parabola from the cell value and the two boundary values.
5. If the parabola has a local extremum within the cell, modify one of the boundary values, so that the extremum falls on a cell boundary.

For the example in Fig. 2, PP performs better than all the other schemes with only a moderate amount of diffusion on the one hand and only a small tendency to form flat tops on the other hand. There is not overshoot or antidiffusion at all.

However, there is a feature in the PP reconstruction in Fig. 1 that one might criticize: the step in the linear slope between cell 3 and 4 is not treated as discontinuity as e.g., by the MinMod scheme, but is modelled by a smoother function that clearly has bumps next to the step. These bumps show up in the solution if such a structure is advected. The monotonicity constraints in the PP scheme prevent the bumps from becoming local extrema. Nevertheless, they are noticeable and might be the cause for some spurious artefacts that can occur when CO5BOLD is used with PP.

To get a second-order method that behaves similar to MinMod near a step in a slope (by taking the curvature of the polynomials into account similar to a WENO scheme, see Shu & Osher 1989), that avoids anti-diffusion like MinMod and PP (by using the preliminary boundary values), and that maintains monotonicity like PP (by catching all cases at which local extrema can occur), the monotonic *Frankenstein's method* (FRmono) was devised and implemented in CO5BOLD – stitched together out of pieces from the three schemes MinMod, PP, and WENO. The reconstruction of a density by a parabola with FRmono can be outlined as:

1. For each cell, compute the parabola that has as integral – taken over the respective intervals – the cell value and the values in the two neighbor cells.
2. At each cell boundary, compute preliminary boundary values by averaging the values of the two parabola that cross the boundary.
3. Make sure that the boundary values lie between the values of the immediate neighbors.
4. If a cell has a local extremum in the discrete cell values, use a constant value as reconstruction in the cell.
5. Otherwise, compute in the cell a candidate parabola as weighted average of the three parabolae (from step 1) that cover the cell in a WENO style. The weight of each parabola is derived from its second derivative.
6. If the difference of the boundary values of the candidate parabola (from step 5) and the cell value itself differs in sign from the difference of the boundary values (from step 3) and the cell value, use a constant value as reconstruction in the cell.
7. If the candidate parabola has a local extremum within the cell, modify the slope (without increasing the curvature much) so that the extremum falls on a cell boundary.
8. If the candidate parabola lies outside the range allowed by the boundary values, modify the slope (without increasing the curvature much) accordingly.

This FRmono scheme has all the required properties resulting in a nice looking reconstruction (cf. Fig. 1) without conspicuous features like antidissipation steps or overshoot. However, it is a bit involved and it is only marginally less diffusive than the much simpler vanLeer scheme (compare the examples in Fig. 2).

To increase the effective resolution some restrictions in item 3 and 7 in the list above were dropped – thus sacrificing strict monotonicity – resulting in the FRweno scheme. It is significantly less diffusive than the vanLeer reconstruction (see Fig. 2), models smooth local extrema better than PP (compare the region between cell 12 and 15 in Fig. 1), and handles a step in the slope (between cells 3 and 4 in

Fig. 1) without the bump – i.e., better than PP. One the downside, it does not preserve fine details quite as well as PP and it is not strictly monotonic anymore. Still, it can handle all test cases done with CO5BOLD so far, including shock tests like the Sedov blast wave problem (cf. Fig. 4). and stellar atmospheres from brown over white dwarfs, to the sun, and even red supergiants (see Sect. 5).

The fact that abandoning strict monotonicity of the reconstruction scheme does not cause any obvious stability problems, hints at the possibility of using a properly chosen WENO scheme instead. However, for the time being, FRweno is the recommended default reconstruction type for CO5BOLD. While FRmono is only an available safe fall-back method, PP could be used to get the highest resolution on a given grid – on the cost of possible small-scale and low-amplitude artefacts.

2.3. Transversal dissipation

Many implementations extend a 1D hydrodynamics scheme to more dimensions in a way that for flows aligned with an axis dissipation occurs only along the direction of motion (see the sketch in Fig. 3), but not perpendicular to it. That would mean for instance for a shear flow aligned with a grid axis that dissipation occurs in the flow direction but not in the shear direction. That poses no immediately obvious stability problem. But the HLL solver, that is used for MHD simulations with CO5BOLD, has some dissipation even without any flow velocity and also for the grid-aligned flows. And it shows a better behavior than the Roe solver for the Sedov blast wave problem (compare the top left panels in Fig. 4 to the rest), at the cost of relatively large dissipation particularly for low-Mach-number flows.

The Sedov blast waves (Sedov 1959) in Fig. 4 were computed on a 2D 51×51 grid for a gas with $\gamma=1.4$ with initially nine cells in the center having 10^5 times the temperature of the homogeneous surroundings (i.e., $E_0=9 \cdot 10^5$). Because the initial density is constant everywhere the central pressure is also enhanced by this factor. That leads to a rapidly expanding – ideally circular – shock wave. Its

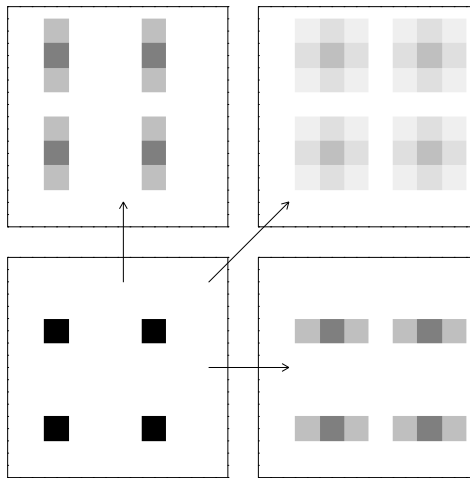


Fig. 3. The initial field (just four filled grid cells) in the lower bottom panel is advected by one grid point in two steps upward (top left panel), diagonally (top right panel), or horizontally (bottom right panel) with a scheme that has only dissipation in the direction of advection. For predominantly horizontal or vertical flows, small-scale structures get aligned with the grid.

temperature and radial velocity field are shown when its radius reaches about 20 grid points for six parameter combinations. Note, that this numerical experiment is meant as a stress test for CO5BOLD and that a smaller-amplitude initial disturbance smoothed over several grid points or a better numerical resolution would give much nicer-looking results.

To make the numerical dissipation in the HD solver of CO5BOLD more isotropic, optional transversal dissipation can now be activated, separately for the internal energy (`C.hydsDiffVelo`) and the transversal velocities (`C.hydvDiffVelo`). This dissipation has only a minor impact on the effective numerical resolution but improves the behavior in test cases like the Sedov blast wave (compare the right panels in Fig. 4). It acts a bit like the previously recommended tensor viscosity but it is now part of the HD solver and acts only on jumps between cell-boundary values after the reconstruction step has been performed.

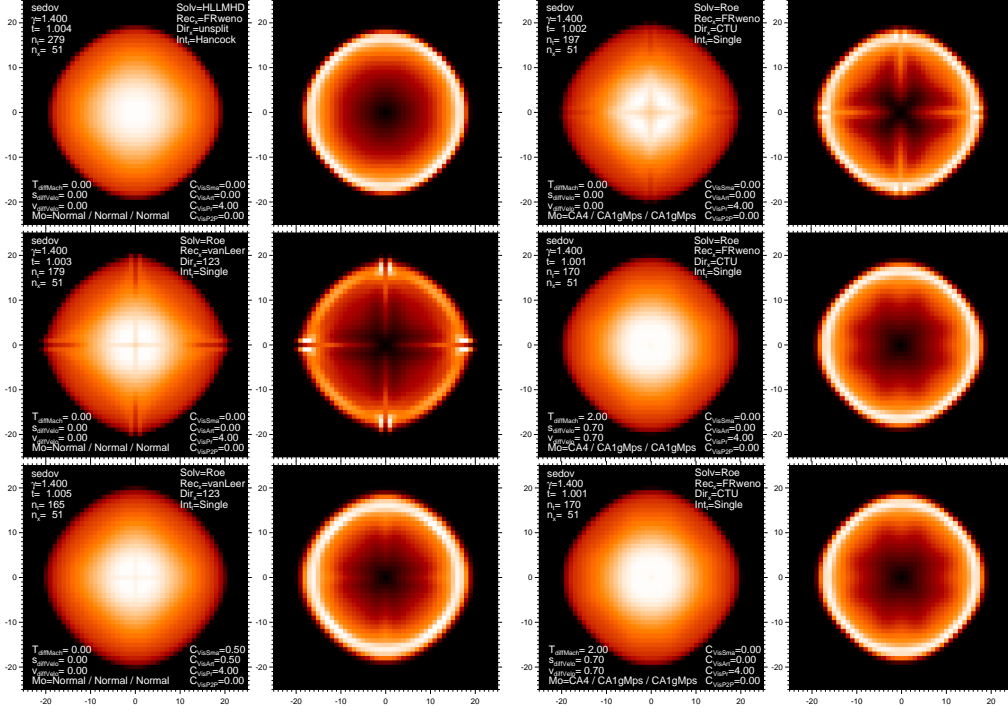


Fig. 4. 2D Sedov blast wave: pairs of temperature (left panel) and radial velocity (right panel) plots for 6 parameter combinations: HLL solver (top left), Roe solver, old version (middle left), Roe solver, old version including tensor viscosity (bottom left), Roe solver, current version (top right), Roe solver, current version including transversal diffusion (middle right), Roe solver, current version including transversal diffusion and tensor viscosity (bottom right). The axis units are grid cell numbers.

2.4. Extra dissipation

With the 1D reconstruction and the transversal dissipation as outlined above many test problems and stellar atmosphere models can be computed. However, there are cases where some additional dissipation can be helpful: to damp transient oscillations more rapidly, to reduce fluctuations in the uppermost/outermost layers (to increase the time step), or to stabilize the interaction of the hydrodynamics solver with the radiation transport in the presence of a gravity field. In particular for simulations of giants (Ludwig & Kučinskas 2012) and supergiants (Freytag et al. 2002), where Mach numbers and opacity fluctuations are large and radiative time scales are comparatively short, some additional measures can be necessary:

Within the HD solver, an extra energy dissipation, that only fills local temperature holes, can be activated with `C_hydTdiffMach`. In the case of strong density gradients, the reconstruction scheme described above can be made more dissipative (by interpolation e.g., FRweno with MinMod) by setting `C_SlopeRed` to a positive value.

Separate from the HD solver, a tensor viscosity can be activated either for the old discretization with parameters like `C_visSmagorinsky`, or for the newer point-to-point discretization with parameters like `C_visP2PCoeff`.

As a last resort, within any of the radiation transport modules nonconservative energy *generation* in case of too low temperatures can be activated with `C_TminLimit`.

3. Waves and averages in the Roe solver

The Roe scheme (Roe 1986) constructs the fluxes of a density (per mass unit) q through a cell boundary as sum of the averages of the fluxes of the left and right adjacent cells

$$f_{\rho q, \text{avg}} = \frac{1}{2} (q_{\text{left}} f_{\rho, \text{left}} + q_{\text{right}} f_{\rho, \text{right}}) \quad (6)$$

and correction terms involving the Roe matrix, whereas consistent advection (Norman & Winkler 1986) would rather use

$$f_{\rho q, \text{avg}} = \frac{1}{4} (q_{\text{left}} + q_{\text{right}}) (f_{\rho, \text{left}} + f_{\rho, \text{right}}) \quad (7)$$

for the averaged flux. Here, f_{ρ} is the mass flux.

3.1. Energy flux

When applied to the enthalpy flux equation, the original Roe formula (6) has to be used for shocks, while Eq. (7) turns out to be superior for small-Mach-number, near-hydrostatic, near-adiabatic conditions. With the parameter `hdEnthalpyAvgMode` the type of averaging or the type of smooth interpolation between both cases can be selected.

For the same reason, there is the possibility to interpolate between the original Roe formula for the correction terms for the entropy wave, which uses the fluctuations in pressure and density, and a version, that uses the entropy fluctuations directly, controlled via `hdEntropyWaveMode`.

3.2. Transversal momentum fluxes

Using a recipe similar to Eq. (7) instead of Eq. (6) for the transversal momentum fluxes improves the behavior of CO5BOLD considerably when solving the Sedov blast wave problem (see Fig. 4). There is no adverse effect in the small Mach numbers. So, with `hdTransVeloMode` the old or the new (recommended) treatment can be selected. There is no interpolation between the cases necessary.

4. Directional splitting and time integration

CO5BOLD now offers several ways of combining the 1D fluxes to advance the solution from time step $^{(n)}$ to $^{(n+1)}$ in two (as in the equations below) or three dimensions. The old standard was “directional splitting” (`hdsplit=123`, `hdTimeIntegrationScheme=Single`), which is fast and robust, but shows some noise under near-incompressible conditions:

$$q'_{i,j} = q_{i,j}^{(n)} - \frac{\Delta t}{\Delta x} (f_x(q_{i+\frac{1}{2},j}^{(n)}) - f_x(q_{i-\frac{1}{2},j}^{(n)})) \quad (8)$$

$$q_{i,j}^{(n+1)} = q'_{i,j} - \frac{\Delta t}{\Delta y} (f_y(q'_{i,j+\frac{1}{2}}) - f_y(q'_{i,j-\frac{1}{2}})) \quad (9)$$

The simple unsplit scheme (`hdsplit=unsplit`, `hdTimeIntegrationScheme=Single`),

$$q_{i,j}^{(n+1)} = q_{i,j}^{(n)} - \frac{\Delta t}{\Delta x} (f_x(q_{i+\frac{1}{2},j}^{(n)}) - f_x(q_{i-\frac{1}{2},j}^{(n)})) \quad (10)$$

$$- \frac{\Delta t}{\Delta y} (f_y(q_{i,j+\frac{1}{2}}^{(n)}) - f_y(q_{i,j-\frac{1}{2}}^{(n)})) \quad (11)$$

where the individual 1D fluxes contain terms of higher-order in Δt , was used e.g., in Freytag et al. (2010). But it is not commended anymore, because the Corner-Transport-Upwind scheme (CTU, see Colella 1990, activated with `hdsplit=CTU`, `hdTimeIntegrationScheme=Single`),

$$q'_{i,j} = q_{i,j}^{(n)} - \frac{\Delta t}{2\Delta x} (f_x(q_{i+\frac{1}{2},j}^{(n)}) - f_x(q_{i-\frac{1}{2},j}^{(n)})) \quad (12)$$

$$q''_{i,j} = q_{i,j}^{(n)} - \frac{\Delta t}{2\Delta y} (f_y(q_{i,j+\frac{1}{2}}^{(n)}) - f_y(q_{i,j-\frac{1}{2}}^{(n)})) \quad (13)$$

$$\Delta q'''_{i,j} = - \frac{\Delta t}{\Delta y} (f_y(q''_{i,j+\frac{1}{2}}) - f_y(q''_{i,j-\frac{1}{2}})) \quad (14)$$

$$\Delta q''''_{i,j} = - \frac{\Delta t}{\Delta x} (f_x(q'_{i+\frac{1}{2},j}) - f_x(q'_{i-\frac{1}{2},j})) \quad (15)$$

$$q_{i,j}^{(n+1)} = q_{i,j} + \Delta q'''_{i,j} + \Delta q''''_{i,j} \quad (16)$$

shows much less numerical artefacts in those situations. It is the currently recommended general default. For very low Mach-number flows, the second-order Runge-Kutta (predictor-corrector) scheme, (`hdsplit=unsplit`, `hdTimeIntegrationScheme=RungeKutta2`), where the individual 1D fluxes don't contain Δt terms,

$$q'_{i,j} = q_{i,j}^{(n)} - \frac{\Delta t}{\Delta x} (f_x(q_{i+\frac{1}{2},j}^{(n)}) - f_x(q_{i-\frac{1}{2},j}^{(n)})) \quad (17)$$

$$-\frac{\Delta t}{\Delta y} (f_y(q_{i,j+\frac{1}{2}}^{(n)}) - f_y(q_{i,j-\frac{1}{2}}^{(n)})) \quad (18)$$

$$q''_{i,j} = q'_{i,j} - \frac{\Delta t}{\Delta x} (f_x(q'_{i+\frac{1}{2},j}) - f_x(q'_{i-\frac{1}{2},j})) \quad (19)$$

$$-\frac{\Delta t}{\Delta y} (f_y(q'_{i,j+\frac{1}{2}}) - f_y(q'_{i,j-\frac{1}{2}})) \quad (20)$$

$$q_{i,j}^{(n+1)} = \frac{1}{2}(q_{i,j} + q''_{i,j}) \quad (21)$$

has some slight advantages.

The schemes require different CFL-numbers, i.e., they advance with different time steps. In addition, the “directional splitting” and the “simple unsplit” scheme need only one flux computation per direction and time step, whereas the other two schemes (CTU and 2nd-order Runge-Kutta) need two. That means that the most simple method, the “directional splitting” scheme, is the most efficient. It was the standard for CO5BOLD for years. And it is still recommended if the Mach numbers are not too low and the efficiency of the hydrodynamics solver is of prime importance (as e.g., for the solar model in Fig. 6), which is rarely the case because the radiation-transport solver consumes most of the CPU time. Nevertheless, the CTU scheme is now the recommended standard for most cases, even if it is computationally more expensive. The Runge-Kutta scheme is the optimum for low-Mach-number flows (e.g., in a brown dwarf model as in Fig. 5, bottom). It has slightly more restrictive time-step requirements than the CTU scheme and is therefore even more expensive than the CTU scheme.

5. Results

Figure 5 compares the entropy fluctuations in two models of a 700 K 2D brown dwarf, computed with the old and the new code version, respectively. The effective temperature is taken from the PHOENIX atmosphere that was used to construct the start model. The actual effective temperature is much lower because of the enormous vertical extent of the dust cloud layers – likely due to the restriction to too small dust grains.

The flow in the gas convection zone (the bottom half of the plots) now looks much more like a scaled down (geometrically and in velocity and entropy fluctuation amplitude) version

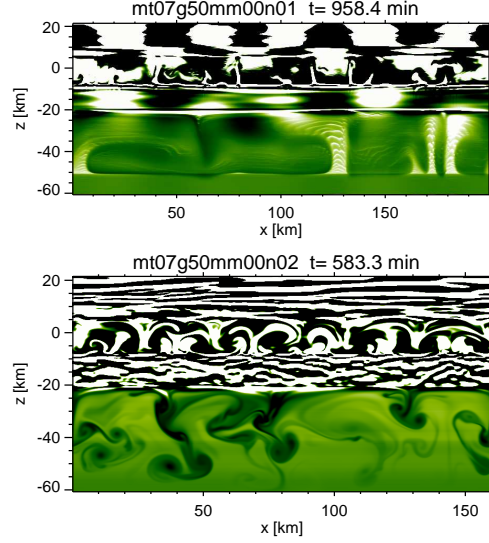


Fig. 5. Entropy fluctuations of a 700 K 2D brown dwarf model with the old (top) and the new (bottom) code version.

of the convective flow in an M dwarf model. It is dramatically less diffusive with a “proper” (i.e., well known from models at higher Mach numbers) mushroom and 2D-turbulence pattern of the cool downdrafts. There are much less artefacts in the upflows, too. The entropy waves (in the top half of the model) have smaller scales. The dust convection zone (around $z = 0$) looks different, too, which is partly due to the fact that the bottom model has been given much more time to relax.

A version of CO5BOLD with many but not all of the new features has been successfully used by W. Schaffenberger to compute global toy models of rotating M dwarfs to determine the effect of rotation on the convective efficiency (see Allard et al. in these proceedings).

The solar model presented in Fig. 6 shows more fine structure in the surface intensity and also in the deep entropy field than previous CO5BOLD models (e.g., Beeck et al. 2012). That is mostly due to the comparably high spatial resolution of $800^2 \times 400$ grid points with a 7 km^3 grid size and the use of the aggressive (i.e., detail-preserving but possibly artefact) piecewise parabolic (PP) reconstruction method. PP was working before but showed

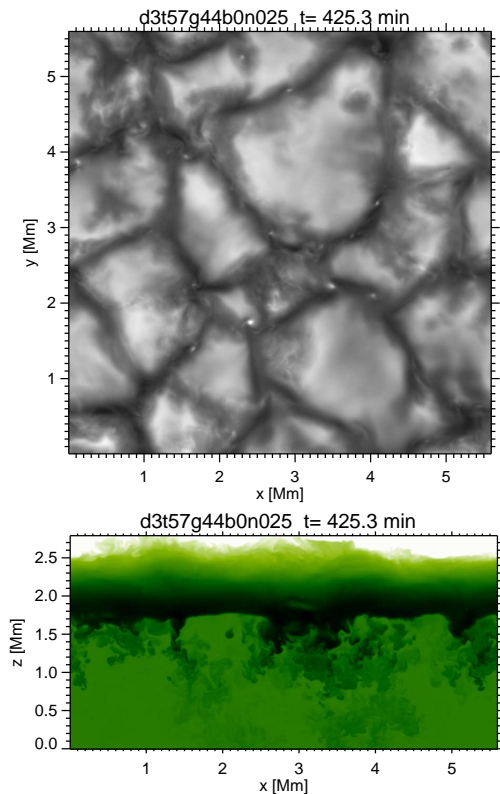


Fig. 6. Emergent grey surface intensity (top) and entropy (bottom) of a 3D solar model with a resolution of $800^2 \times 400$ grid points and the PP reconstruction that reveals lots of fine structures including the bright centers of vortices.

small-scale spikes in the velocity and entropy fields, that are now gone. A significant contribution of the effective increase in resolution comes from the absence of any additional tensor viscosity in the new model. This viscosity was previously activated by default, e.g., also in the CO5BOLD solar reference model in Beeck et al. (2012).

6. Conclusions

The overhauling of many aspects of the Roe solver used in the hydrodynamics module of CO5BOLD results in a significantly better behavior at low Mach numbers, and an improved stability at larger Mach numbers requiring less

(or no) additional tensor viscosity, which then leads to a noticeable increase in effective resolution.

Acknowledgements. The project was financed by the Agence Nationale de la Recherche (ANR), and the Programme National de Physique Stellaire (PNPS) of the Centre National de Recherche Scientifique (CNRS). The computations were performed at the Pôle Scientifique de Modélisation Numérique (PSMN) at the École Normale Supérieure (ENS) in Lyon.

References

- Beeck, B., Collet, R., Steffen, M., et al. 2012, *A&A*, 539, A121
- Colella, P. 1990, *J.Comp.Phys.*, 87, 171
- Colella, P. & Woodward, P. R. 1984, *J.Comp.Phys.*, 54, 174
- Freytag, B., Allard, F., Homeier, D., Ludwig, H., & Steffen, M. 2011, in *Astronom. Soc. of the Pacific Conf. Series*, ed. J. P. Beaulieu, S. Dieters, & G. Tinetti, Vol. 450, 125
- Freytag, B., Allard, F., Ludwig, H.-G., Homeier, D., & Steffen, M. 2010, *A&A*, 513, A19
- Freytag, B. & Höfner, S. 2008, *A&A*, 483, 571
- Freytag, B., Steffen, M., & Dorch, B. 2002, *Astron. Nachr.*, 323, 213
- Freytag, B., Steffen, M., Ludwig, H.-G., et al. 2012, *J.Comp.Phys.*, 231, 919
- Harten, A., Lax, P. D., & van Leer, B. 1983, *SIAM Review*, 25, 35
- Ludwig, H.-G. & Kučinskas, A. 2012, *A&A*, 547, A118
- Norman, M. L. & Winkler, K.-H. A. 1986, in *Astrophysical Radiation Hydrodynamics*, ed. K.-H. A. Winkler & M. L. Norman, 187
- Roe, P. 1986, *Annu. Rev. Fluid Mech.*, 18, 337
- Sedov, L. I. 1959, *Similarity and Dimensional Methods in Mechanics* (New York: Academic Pres)
- Shu, C.-W. & Osher, S. 1989, *J.Comp.Phys.*, 83, 32
- Steffen, M. & Freytag, B. 2007, *Astron. Nachr.*, 328, 1054
- Steffen, M., Ludwig, H.-G., & Caffau, E. 2009, *Mem. Soc. Astron. Italiana*, 80, 731
- van Leer, B. 1979, *J.Comp.Phys.*, 32, 101